Journal of Materials Chemistry A

Accepted Manuscript

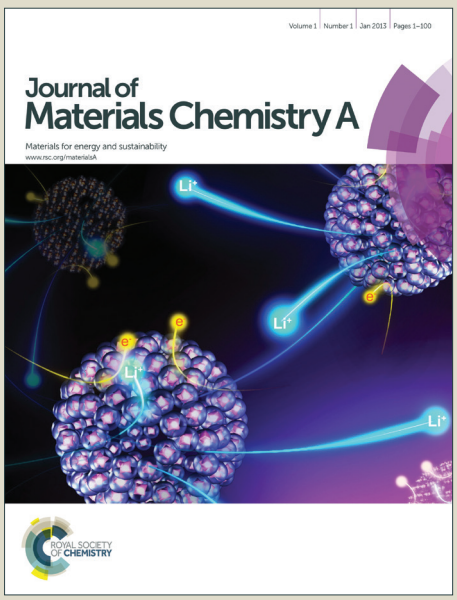

ROYAL SOCIETY OF CHEMISTRY

www.rsc.org/materialsA

Polymer-bound antioxidants in grafted membranes for fuel cells

Yves Buchmüller, Alexander Wokaun, Lorenz Gubler*

Electrochemistry Laboratory, Paul Scherrer Institut, CH-5232 Villigen PSI, Switzerland

Graphical Abstract

Antioxidants are covalently attached to the polymer backbone in radiation grafted fuel cell membranes. The obtained membranes displayed superior stability compared to non-stabilized membranes.

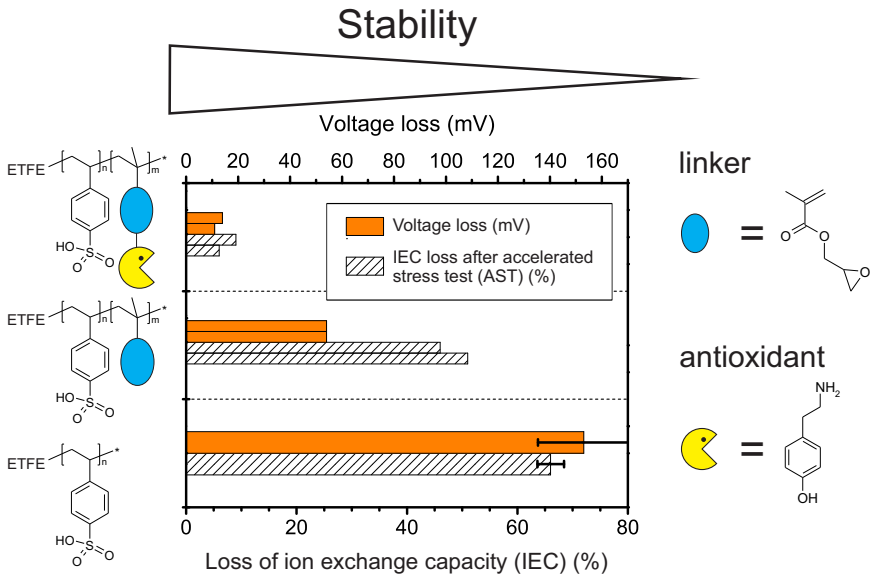

Polymer-bound antioxidants in grafted membranes for fuel cells

Yves Buchmüller, Alexander Wokaun, Lorenz Gubler*

Electrochemistry Laboratory, Paul Scherrer Institut, CH-5232 Villigen PSI, Switzerland

*Corresponding author. Tel.: +41-56-3102673; fax: +41-56-3104416.

E-mail: lorenz.gubler@psi.ch

Abstract

Proton conducting membranes for fuel cells containing antioxidants were synthesized by radiation grafting. Styrene and a “linker” monomer were pre-irradiation cografted into ETFE base film of 25 μm thickness. Tyramine, a phenol type antioxidant, was subsequently covalently attached to the “linker” units, and the styrene units were sulfonated. FTIR and SEM-EDX analysis of the synthesized films and membranes was performed to confirm uniform grafting, functionalization and sulfonation steps. The obtained membranes were characterized in terms of ion exchange capacity (IEC), water uptake and through-plane conductivity. The cografted membranes were assembled into a fuel cell and tested under accelerated aging conditions to assess their chemical stability. The membranes containing the tyramine moieties degraded substantially less compared to membranes lacking these phenolic groups. *Post-test* FTIR and IEC analysis confirmed the results of the fuel cell test, which supports the notion that the polymer-bound antioxidants effectively mitigate oxidative aging of the polymer electrolyte in a fuel cell.

Keywords: Fuel Cell, Proton Exchange Membrane, Radiation Grafting, Glycidyl Methacrylate (GMA), Vinylbenzyl Chloride (VBC), FTIR, SEM EDX, Phenol Type Antioxidant, Tyramine

Introduction

Polymer electrolyte fuel cells (PEFCs) are clean and efficient electrochemical energy conversion devices. They are typically operated at temperatures ranging from 50 to 80°C. The heart of the PEFC is the membrane electrode assembly (MEA), consisting of the proton exchange membrane sandwiched between gas diffusion electrodes comprising noble metal catalyst. State-of-the-art-membranes are perfluorosulfonic acid (PFSA) polymers (Nafion®, Flemion®, Aciplex®, etc.) due to their encouraging performance and durability. However, the fluorine chemistry involved in the preparation of PFSA materials is a drawback: hazardous intermediates and processing steps with low yield increase the production costs of these kinds of materials compared to non-fluorinated polymers.[1, 2]

An alternative to PFSA membranes are pre-irradiation grafted membranes. A commercially available basefilm is electron beam activated and grafted with monomers. The grafted chains can be post-functionalized and post-sulfonated to introduce desired material properties.[3] A advantage compared to PFSA membranes is the versatility of the synthesis: a wide choice of base materials and monomers is avialable and applied for a range of applications in different fields, e.g., filter and separation applications,[4] water treatment[5] and fuel cells.[6, 7] Grafting of monomers into a basefilm is a diffusion and reaction controlled process.[8, 9] If the diffusion of the monomers into the film is faster than the polymerization reaction, grafting occurs quasi simultaneosly throughout the film, whereas, in the opposite case, the grafting takes place on the surface of the film initially, and only with time the inner portions of the base film are grafted. The latter case is referred to as "front mechanism".[9]

Radiation grafting of styrene into poly(ethylene-*alt*-tetrafluoroethylene) (ETFE) and other base films with subsequent sulfonation of the polystyrene grafts has been applied to

prepare proton exchange membranes for fuel cells, i.e., ETFE grafted with polystyrenesulfonic acid (ETFE-*g*-PSSA).[3] The choice of monomers, however, is not restricted to styrene, other (co)monomers can be grafted and sulfonated. For example, proton conducting membranes based on cografted styrene and methacrylonitrile were prepared and tested in our group. This type of membrane showed a promising long term stability compared to pure styrene based membrane materials.[10]

Membrane degradation in the fuel cell and failure is a factor limiting the lifetime of the membrane electrode assembly.[11] It can generally be divided into mechanical and chemical degradation. Mechanical degradation is typically caused by induced internal mechanical stress as a result of changing water content of the ionomer during the varying conditions in the fuel cell. Chemical degradation occurs when the polymer is decomposed or its constituent chains are repeatedly cleaved. Chemical degradation of the membrane during fuel cell operation is caused by reactive intermediates present in the membrane, such as hydroxyl radicals ($HO^{\bullet}$).[11-13] They react with the membrane material and alter its chemical structure, which can lead to decomposition of the chains. It is still under debate whether the hydrogen peroxide decomposition is the main source of radicals or direct production of the radical species on the catalyst in presence of hydrogen and oxygen is the dominating pathway.[14-17] However, gas crossover is an important factor for the generation of these reactive intermediates: the higher the crossover the more decomposition products of the membrane are found in the exhaust water.[15, 17, 18]

One effective mitigation strategy against chemical degradation of PFSA membranes consists of introducing redox active transition metal ions or their corresponding oxide into the PFSA materials, e.g. Ce(III)[12, 13] or MnO_2.[14, 19] Accelerated fuel cell tests show significantly lower degradation rates for PFSA membranes containing these redox

couples.[13-15, 19] This is attributed to the free radical scavenging activity of the incorporated metal ions. They react with $HO^{\bullet}$, which leads to a reduction of the chemical attack on the membrane. In addition, in the case of cerium, it has been proposed that the scavenging mechanism is regenerative.[13] The regeneration of Ce(III) is explained by reaction of Ce(IV) ions with H_2O_2 and $HO_2^{\bullet}$ radicals, which reduces the cerium ion back to its "radical scavenging state". A similar regenerative mechanism is conceivable in the case of manganese. This is supported by a recently published kinetic modeling study.[16] However, the authors of that work argue against incorporating Ce ions into membranes containing aromatic groups due to possible attack of aromatic structures by Ce(IV). Another reason, according to the authors, is the higher affinity of aromatic structures to react with radicals compared to aliphatic structures of PFSA type membranes: the calculations show that high cerium concentrations are required to bring about a stabilizing effect. This is a result of the high concentration of aromatic groups in polyarylene materials or styrene containing radiation grafted polymers, and the rate constant for the reaction of radicals with aromatic units is two orders of magnitude higher compared to rate constant of the reaction with PFSA ionomer.

Degradation of PFSA materials due to radical attack was extensively investigated during the past ten years,[11, 17, 18, 20-22] whereas for grafted or other alternative membranes fewer studies have been published. Hübner and Roduner conducted an ESR study on radical attack on a model compound for sulfonated polystyrene in 1999.[23] Only one group did similar work on oligomers of sulfonated styrene to gain more insight into degradation mechanisms of PSSA based membranes.[24-27] These publications suggest degradation pathways to benzylic radicals, which lead to chain scission and, consequently, to loss of the grafted chains and the attached sulfonic acid groups. This leads to decreasing proton conductivity and, eventually, to the complete loss of proton exchange sites in the material.

Possible strategies to mitigate chemical degradation of grafted membranes are: lowering reactant gas crossover[20, 28] of grafted membranes by improving the gas barrier properties[29] and use of intirinsically more stable monomers, e.g., α-methylstyrene, in which the weak α-position is protected by a methyl group.[30] An alternative is to introduce radical scavengers. Organic radical scavengers are applied in the plastics industry to increase the lifetime of the products.[31] An efficient class of these antioxidants is hindered phenols, owing to their high radical scavenging activity.[16, 31, 32] Grafted membranes could be doped with organic radical scavengers to prevent or reduce chemical attack of the grafted aromatic chains. Unfortunately, during fuel cell operation, water is dragged through the membrane by electroosmosis, which could wash out non-covalently attached radical scavenging molecules.

It is conceivable to covalently attach radical scavenging molecules to the polymer due to the versatility of the grafting method. Cografting of different monomers is well known.[5, 6] Two general approaches to covalently attach antioxidants (AOs) suggest themselves for grafted PSSA type membranes: either the AO is direclty cografted with styrene, or it is introduced after the grafting by a polymer-analogous substitution reaction with a suitable cografted linker. The choice of low-cost polymerizable AOs is very restricted. This suggests the synthetic route via cografting of styrene and linker monomers and post-functionalization of the linker to introduce the AO.

Possible linkers include vinylbenzyl chloride (VBC) and glycidyl methacrylate (GMA). Grafting of VBC onto different base materials has been known since the 1980s.[33-36] Applications include heavy ion separation and chromatography after post-phosphonation of the grafted VBC. More recently, VBC was grafted onto ETFE by Slade and Varcoe to synthesize anion exchange membranes by post-functionalizing the grafts with amines.[37-40]

Schmidt-Naake and coworkers grafted VBC onto ETFE to produce proton exchange membranes via phosphonation of the grafted chains.[41, 42] GMA was recognized as an interesting monomer for grafting since the mid-1960s.[43-45] Among others, a group at the Japan Atomic Energy Agency (JAEA) grafted GMA onto different porous polymers to produce metal-ion adsorbents.[46] The versatility of grafted GMA was demonstrated by various post-functionalizion reactions of the pendant epoxy groups in the graft copolymer (sulfonation, phosponation, amination, reaction with H_2S).[4, 45, 46] The functionalized membranes adsorb different metal ions with high specificity, depending on the type of introduced functional group.[4] These membranes are intended to be applied in waste-water treatment and heavy metal ion removal. The use of materials grafted with GMA in filtration and separation applications is described in a recent review on radiation-grafted membranes for purification and separation purposes.[4]

In principle, copolymerizable monomers can be cografted into a suitable basefilm.[8, 47] In the case of VBC, cografting with styrene onto polystyrene based material was published by Revillon and coworkers as early as 1989.[48] The group around T. Sugo cografted VBC and styrene to produce membranes containing both, phosphonic and sulfonic acid groups.[49] For GMA, to our best knowledge, only one group published cografting of styrene with GMA.[50] Interestingly, they tried to synthesize a proton exchange membrane for application in fuel cells by sulfonating both, the GMA and the styrene units in the grafted chains.

(Scheme 1)

To our best knowledge, the use of GMA and VBC as linker comonomers to covalently attach potential radical scavengers has not been reported so far. This study presents two synthetic routes to attach a phenolic radical scavenger to PSSA based membranes for fuel

cells. Tyramine is used as a potential radical scavenger and attached to the linker in a post-grafting functionalization reaction (Schemes 1 and 2). The grafted films and membranes were characterized qualitatively and quantitatively using using transmission FTIR spectroscopy. Relevant *ex situ* data are presented (graft level, ion exchange capacity, conversion of the functionalization reaction, degree of sulfonation, swelling, and proton conductivity). The homogeneity of the grafted membranes was analyzed using SEM/EDX by visualizing the distribution of the elements present in the material. Such potentially chemically stabilized membranes were tested in a single cell setup under open circuit voltage (OCV) conditions, which accelerate chemical degradation,[29, 51, 52] and compared to different non-stabilized PSSA based membranes. No Fenton's tests were performed to assess the chemical stability of the novel membrane materials, because the correlation to the stability in the fuel cell is not straightforward. For instance, Sethuraman and coworkers showed that membranes which display poor stability in the Fenton test as compared to perfluorinated membranes (e.g., Nafion®) may show superior stability during rapid chemical aging testing in the fuel cell at OCV.[53] Polarization curves were taken before and after the accelerated tests to assess *in situ* performance losses, hydrogen permeation was measured electrochemically and the high frequency resistance was recorded during the experiments. Additionally, the membranes were characterized after the fuel cell test by means of FTIR and titratrion to provide complementary data to the *in situ* results and quantify the extent of degradation of the membranes.

(Scheme 2)

Materials and Methods

Chemicals

ETFE (Tefzel® 100LZ) films of 25 µm thickness, purchased from DuPont de Nemours (Circleville, USA), were used as base material. The reagents used were styrene (98%, Fluka), 2-propanol (PROLABO®, VWR), dichloromethane (PROLABO®, VWR), methanol (NORMAPUR®, VWR), acetone (PROLABO®, VWR), dimethyl formamide (DMF, 99.5%, Merck), chlorosulfonic acid (98%, Fluka), glycidyl methacrylate (GMA, 97%, Merck), vinylbenzyl chloride (VBC, >90%, Fluka) and tyramine (99%, SAFC). The stabilizing agent in GMA (monomethyl ether hydroquinone) was removed directly prior to use, using an inhibitor remover column (Sigma-Aldrich), whereas the inhibitor in VBC (4-tertbutyl catechol) was removed by basic extraction in 1 M NaOH(aq). All other chemicals were used as received.

Hydrogen, oxygen and nitrogen (*Messer*, Lenzburg, Switzerland) of a purity of at least 4.5 were used as received.

Instruments

All FTIR spectra were recorded with a PerkinElmer FTIR System 2000. Interpretation and curve fitting was done using GRAMS/386 software (version 3.02) from Galactic Industries.

Acid-base titrations were performed using an SM Titrino 702 from Metrohm (Herisau, Switzerland). Impedance measurements were performed using a Zahner IM6 (*Zahner Messtechnik*, Kronach, Germany). A thickness gauge (MT12B, Heidenheim, Germany) was used to determine the thickness of the respective films and membranes.

All scanning electron micrographs were taken with a FE-SEM Ultra 55 (*Carl Zeiss*, Oberkochen, Germany). Energy dispersive X-ray analysis was performed using a compatible accessory (EDAX TSL, AMETEK).

During fuel cell operation, the high frequency resistance of the cell was continuously measured at 1 kHz with an AC milliohm meter model 3566 from Tsuruga (Osaka, Japan).

Experimental

Grafting

The ETFE film was cut into pieces of 20 by 20 centimeters. Before irradiation, the samples were washed in ethanol and dried in vacuum at 60 °C. They were electron beam irradiated under air with a dose of 1.5 kGy for styrene grafting, 15 kGy for GMA and GMA / styrene and 30 kGy for VBC and VBC / styrene grafting (MeV range accelerator)[54, 55] at Leoni-Studer AG (Däniken, Switzerland). Subsequently, the films were stored at -80 °C until used.

All grafting reactions were carried out in glass reactors (3 cm diameter, 18 cm height, 50 ml capacity) under nitrogen atmosphere, using 6 cm * 9 cm pre-irradiated ETFE films. The grafting solution was added and degassed for one hour by purging with nitrogen. Then the reactors, containing the films and the grafting solution, were placed in a thermostatic water bath at 60 °C for different times. The grafted films were extracted with different solvents overnight to remove residual monomer and/or homopolymer, then dried at 80 °C under vacuum and reweighed. All details for the different grafting reactions are given in Table 1.

(Table 1)

The graft level (GL) of each film was determined from the weights of the irradiated (W_0) and grafted film (W_g), respectively:

$$GL = \frac{W_g - W_0}{W_0} \cdot 100\,\% \qquad (1)$$

For cografted films, the respective content of the individual monomer units in the grafted chains was determined by FTIR analysis. In principle, chemical analysis can be done quantitatively without the need for calibration measurement series using NMR spectroscopy. However, since ETFE and the derived grafted polymers are not soluble in any known solvent, solid-state NMR spectroscopy has to be used. We have used solid-state NMR spectroscopy initially to qualify the FTIR method.[56] Also, if distinct vibrational bands are not present or not well resolved for certain graft components, solid-state NMR can be used for characterization.[57] For quantitative compositional anaylsis using transmission FTIR spectroscopy, in a first step a calibration curve was established: grafted films of one monomer (e.g. ETFE-*g*-PS) at different graft levels were analyzed by FTIR spectroscopy. Integrals of bands assignable to the grafted monomers were normalized to the bands of ETFE, yielding a linear dependency of these normalized bands to the graft level. Having calibration curves for both cografted monomers provides a powerful analytical tool to spectroscopically determine the relative graft level of the respective grafted monomers, because it decreases the systematic error compared to direct calculation of the components without normalizing to a base film relevant vibrational band. A more detailed description of this methodology is given elsewhere.[58, 59]

Functionalization of the grafted films was performed using a 0.25 M solution of tyramine in DMF / water mixture (9/1 v/v). The grafted films were placed in the glass reactors described above, and, after adding the tyramine solution, purged with nitrogen for 1h. The reactors were closed and placed in a thermostatic water bath at 80°C for 12 h. After the reaction, the functionalized films were washed in acetone overnight to remove residual tyramine and DMF (Scheme 2). After drying the funcionalized films at 80°C under vacuum, they were weighed and the conversion of the tyramination reaction was determined using the following expression:

$$conversion = \frac{(W_{\text{functionalized}} - W_{\text{basefilm}} \cdot (1 + GL_{\text{linker}})) \cdot M_{\text{linker}}}{(M_{\text{functionalized linker}} - M_{\text{linker}}) \cdot GL_{\text{linker}} \cdot W_{\text{basefilm}}} \cdot 100\% \quad (2)$$

Where *W* is the weight of the base film and the grafted and functionalized film, respectively, and *M* is the molar mass of the linker and the functionalized linker respectively. GL_{linker} stands for the spectroscopically determined graft level of the linker (VBC or GMA) in cografted films and the graft level for films grafted with the linker only.

Sulfonation of all styrene containing films was performed in a glass reactor using 2% (v/v) chlorosulfonic acid in dichloromethane at room temperature. The films were carefully placed in the solution in batches of six films maximum. After carefully removing possible air bubbles using a glass rod the reactor was closed and protected with a PVC shielding. After five hours of reaction the sulfonated films (now membranes) were washed thoroughly with ultra-pure water. After keeping the membranes immersed the water was exchanged and the samples were treated at 80°C overnight to hydrolyze the chlorosulfonic to sulfonic acid groups. More detailed information for the grafting and sulfonation procedures for styrene (ETFE-g-PSSA)[3, 54]) and GMA (ETFE-*g*-PGMAS)[60, 61] can be found elsewhere.

Bulk properties (ex situ)

All FTIR spectra were recorded in transmission mode. To minimize the water bands, the sulfonated films were potassium exchanged (immersion in 1M KCl (aq) overnight) and dried in vacuum at 80 °C before measuring.

Ion exchange capacity (IEC), proton conductivity, water uptake and hydration number were determined by acid-base titration, impedance spectroscopy and gravimetrically, respectively, using in-house methods.[62]

The ion exchange capacity (IEC) is defined as

$$IEC = \frac{n(\mathrm{H}^+)}{W_{\mathrm{pol}}} \tag{3}$$

where $n(H^+)$ represents the number of protons (obtained by titration) and W_{pol} the dry weight of the membrane. The water uptake is obtained according to

$$water\ uptake = \frac{W_{\mathrm{wet}} - W_{\mathrm{dry}}}{W_{\mathrm{dry}}} \cdot 100\,\% \tag{4}$$

where W_{wet} and W_{dry} represent the weight of the membrane in wet and dry state, respectively. The samples of sulfonated films for SEM/EDX were potassium exchanged, frozen in liquid nitrogen and fractured to analyze the cross-sections of the membranes.

Calculation of the theoretical IEC is based on the assumption of one sulfonic group per styrene unit and is described by equation (5):

$$IEC_{theo} = \frac{GL_{\mathrm{tot}}}{M_{\mathrm{styrene}} + M_{\mathrm{comonomer}} / R_{\mathrm{m}} \cdot (1 + GL_{\mathrm{tot}}) + M_{\mathrm{SO_3H}} \cdot GL_{\mathrm{tot}}} \tag{5}$$

Where GL_{tot} is the graft level of the cografted film and M is the molar mass. R_m indicates the molar ratio of styrene and comonomer, which is defined as

$$R_m = \frac{n(\text{styrene})}{n(\text{comonomer})} \quad (6)$$

A more detailed explanation on this calculation can be found elsewhere.[63]

Fuel cell tests (in situ)

Selected styrene based membranes of a graft level of ~23% were tested as a reference. They were laminated with JM ELE162 gas diffusion electrodes (loading: 0.4 mg Pt/cm^2, Johnson Matthey Fuel Cells, Swindon, UK) by hot-pressing (110 °C / 2.5 MPa / 180 s) to form a membrane electrode assembly (MEA).[64]

All other single cells were assembled using air-dried membranes sandwiched between two JM ELE162 electrodes. The active area of the single cell used for all fuel cell tests is 16 cm^2, the flow field channels are parallel. Further details of the utilized single cell are given elsewhere.[65]

The *in situ* characterization of the MEAs by polarization curves and hydrogen crossover measurements was performed using in-house methods.[64] The MEAs were preconditioned for 1 h under nitrogen and hydrogen. The hydrogen permeation was determined using an electrochemical method.[64] Then, the MEAs were conditioned in constant current mode (0.5 A/cm^2) at 80°C, using pure oxygen and hydrogen (100 % relative humidity). The gases were fed at a flow rate of 600 ml/min each and at a pressure of 2.5 bar$_a$. The high frequency resistance was continuously measured at 1 kHz.

After conditioning of the MEA the first polarization curve was measured and the cell was switched to open circuit voltage (OCV) for 4h. Then, after 10 minutes of conditioning at constant current (0.5 A/cm^2), the second polarization curve was measured. The cell was switched back to OCV and the gases changed to hydrogen and nitrogen for 1 h to measure the hydrogen permeation after completion of the degradation protocol.

Results and Discussion

Grafting of styrene and linkers into ETFE

The kinetics of pre-irradiation grafting of styrene, VBC and GMA into ETFE, respectively, are given elsewhere.[54, 60, 66]. Cografting kinetics of GMA and S (molar ratio of 0.46 / 0.54) under the given conditions (see Table 1) are represented in Figure 1. A logarithmic dependence of the graft level on the grafting time was found. This can be explained by a decreasing number of radicals available for polymerization of grafted chains over time[67]. The grafting reaction is rather fast compared to the cografting of VBC and S: cografting of GMA and styrene yields practical graft levels of around 50 % within hours, whereas for VBC and S, the synthesis takes around 20 h. The obtained grafting kinetics of GMA and S cannot be compared to existing ones because Abdel-Hady and coworkers did not show kinetic data.[50]

(Figure 1)

The content of S and GMA in the grafted chains was determined using the above mentionend FTIR method.[58, 59] The calculated values for the combined graft level (GL_{tot} (FTIR)) of the cografted films are given in Table 2. They are close to the gravimetrically determined values for the analyzed films. As the deviation of the calculated

GLs is rather small, the method can be considered sufficiently accurate. The obtained values for GL_{GMA} (FTIR) are used below to determine the conversion to the functonalized (tyraminated) films.

(Table 2)

For ETFE cografted with S and VBC the superposition of the IR-bands of S and VBC makes it difficult to use the bands of VBC for quantification. Both S and VBC have aromatic skeleton vibrations and aromatic C-H stretch vibrations. As a consequence, the determination of the molar fraction of S in the cografted films was performed using baseline separated bands of S (1493 cm^{-1} and 761 cm^{-1}) grafted onto ETFE (1324 cm^{-1} and 509 cm^{-1}). The determined molar fraction of S in the grafts is 55.5 ± 0.9 mol%. This value was used for the determination of the conversion of benzylic chloride to benzylic amine in ETFE-*g*-P(S-*co*-VBC). In addition to the conversion (or not) to the tyraminated film, an HCl elimination reaction could theoretically occur and is indicated based on elemental analysis for cografted films as well as for films after functionalization, in that a lower content of Cl compared to the theoretical value is found in all cases.

All films were of milky color after grafting. Nevertheless, they were flexible for all analyzed GLs.

Functionalization of the linkers with tyramine

The conversion to the tyraminated linker was determined gravimetrically using Equation 2. First, the functionalization was performed with films grafted only with the linker to clarify whether the synthetic route is possible or not. Tyramination of all films was performed using a 0.25 M solution of tyramine in DMF. Conversion of the amination reaction of different films is summarized in Table 3.

(Table 3)

The VBC grafted films showed a higher conversion for the tyramination compared to co-grafted fims of VBC and S (57% vs. 25%). Most of the articles on functionalization of grafted VBC report bulk amination reactions in aqueuos environment, applying a synthetic pathway via quaternization of the amine.[37-39] The reaction with amine to ammonium renders the material hydrophilic during the reaction. The amination presented here does not lead to a quaternized amine, thus water cannot be used as solvent. An amination reaction with similar conversion for reaction of PVBC with primary amines (54% and 64%) was recently reported.[68] The shown amination reaction was performed out of a DMF solution, similarly to the reaction reported here. The different degrees of conversion for VBC grafted and VBC / S cografted films may be due to the lower swelling capability of DMF for cografted films compared to VBC only grafted films. VBC is more polar compared to styrene, consequently the polar solvent DMF may swell cografted films substantially less, leading to a decreased access of tyramine to the sites of reaction, i.e., the benzylic chloride. No substantial change in the degree of conversion was observed by increasing the time of reaction from 12 to 24 h. Additionally, the swelling of cografted, functionalized and sulfonated films is lower for VBC containing membranes compared to GMA containing ones or pure styrene grafted membranes. This could be explained by a di-functionalization of the primary amine of tyramine, leading to a crosslinked structure. In case of complete di-functionalization of the amine, the conversion would roughly be halved, which is the case here. Unfortunately, the FTIR spectra are not conclusive in this respect. Qualitatively, however, the FTIR spectra suggest the presence of both, secondary and tertiary amines (see Figure 2) according to the bands at 3650 and 3200 cm^{-1}.[69]

(Figure 2)

For GMA grafted and GMA / S cografted films, respectively, there is no substantial difference in conversion (57% vs. 59%). A possible explanantion could be the polar GMA molecule compared to the less polar, aromatic VBC, as swelling of the films strongly depends on the affinity of swelling agent and film material. Additionally, the ester group of GMA may facilitate the access of tyramine in DMF (being an amide and bearing a carbonyl group) to the reactive sites (epoxy group of GMA) in the cografted films. No substantial change in the conversion was observed by increasing the time of reaction from 12 to 24 h. No di-functionalization of the amine, and thus crosslinking, was observed for GMA containing films. This will be considered in the discussion of the fuel cell tests of these materials.

All films are flexible after functionalization and of yellowish color. For GMA containing films, the transparency increases after the tyramination step, whereas the VBC containing ones remain opaque, only changing from whiteish to yellowish color.

Sulfonation of the different cografted and functionalized films

The sulfonation was performed using 2 % (v/v) chlorosulfonic acid in dichloromethane (DCM). This concentration was chosen to avoid excessively harsh sulfonation conditions, which could potentially induce degradation of the linkers (e.g. hydrolysis of the ester in GMA).

The conversion of the sulfonation reaction of styrene grafted films of comparable GLs under these conditions is close to 100%.[70] Elemental analysis (cf. Supplementary Information) of the sulfonated and tyraminated membranes based on VBC as linker, VBC(Tyr), suggests a very high conversion to sulfonated styrene groups in the grafted chains of about 200%, corresponding to two sulfonic acid groups per styrene unit. This is unlikely for electronic and steric reasons. An alternative explanation would be sulfonation

of other (aromatic) groups, either of the linker VBC, the tyramine, or both. Clarification of this using FTIR is unfortunately not possible because of superposition of the aromatic bands of styrene, VBC and tyramine. At the same time, the obtained values for the ion exchange capacity (IEC) of around 1.6 mmol/g are lower than expected for cografted films of this type (theoretically 1.9 mmol/g). This suggests a lower degree of sulfonation than expected, in contradiction to the mentioned elematal analysis results. An explanation for these findings could be a condensation reaction of sulfonic acid units to form sulfone groups. They contain sulfur but no acidic proton. This is not likely to happen at the low temperatures used during synthesis and sulfonation of this material. This discrepancy is currently unresolved.

Representative FTIR spectra of ETFE basefilm, ETFE cografted with styrene and VBC, functionalized cografted film and functionalized and sulfonated ETFE-*g*-P(SSA-*co*-VBC(Tyr)) are given in Figure 2. After grafting, bands around 3000 cm^{-1} (C-H stretch vibrations) confirm the grafting of VBC and styrene. After the amination with tyramine, new bands at higher wavenumbers appear, indicating the presence of N-H strech (from amine) and O-H stretch vibrations from the aromatic alcohol of tyramine. After the sulfonation step, new bands appear at 1009 cm^{-1} and 835 cm^{-1}. They can be attributed to SO_2 symmetric stretch and S-O stretch vibrations of aromatic sulfonic acid, and thus confirm sulfonation of the styrene grafts. The vibrational band of SO_2 at 1009 cm^{-1} is also found for grafted and sulfonated styrene and α-methylstyrene.[71-73]

(Table 4)

For cografted GMA and styrene, the behavior after sulfonation is closer to the expectations. The theoretical IEC values for the different graft levels of ETFE-*g*-P(SSA-*co*-GMA(Tyr)) (35% and 55%) are 1.66 mmol/g and 2.08 mmol/g, respectively, when grafted

out of a S to GMA monomer ratio of 0.73 / 0.27 (n/n). This is in very good agreement with the obtained values of 1.62 and 1.99 mmol/g (see Table 4). This corresponds to a degree of sulfonation of 98% and 96%, respectively. The elemental analysis yields a degree sulfonation of 95% (based on the sulfur content) for both graft levels, which is in very good agreement with the values found by titration. The slight overestimation with the titration method may be because of "overshooting" of the pH 7. Comparison to the data of Abdel-Hady and coworkers is difficult.[50] They find very low degrees of sulfonation: for a membrane of a GL of 36%, they find an IEC value of 0.77 mmol/g. The theoretical IEC for that membrane should be around 1.6 mmol/g (based on complete sulfonation of the styrene units only). As they graft out of a monomer mixture with the same molar ratio, they should have a molar ratio in the grafts comparable to the values reported here. The authors claim sulfonation of both, the styrene and the GMA units in the grafted chains. As a consequence, they should find IEC values even higher than 1.6 mmol/g. Unfortunately, they provide only FTIR spectra of the cografted films and no spectra of the sulfonated membranes. The provided SEM images are not conclusive, since only surfaces of membranes were analyzed and no elemental distribution is given. Explanation of their findings is even more difficult, as they use a harsher hydrolysis environment: the epoxy group of GMA is probably openened to yield the diol during either the basic (0.5M KOH(aq) overnight) or the acidic treatment (boiling in 1M HCl(aq) for several hours) after sulfonation. After these steps it is very unlikely to still find epoxy groups to sulfonate. The FTIR spectrum of the cografted and tyraminated films (Figure 3) shows absence of epoxy groups after the functionalization, which was performed under mild conditions. The authors give no evidence for intact epoxy groups after the sulfonation of the styrene units in the co-grafted and partially sulfonated films. This would be partial explanation of the low IEC

values they find. Still, as mentioned above, they find a degree of sulfonation of the styrene units below 50%.

(Figure 3)

In Figure 3, representative FTIR spectra of ETFE basefilm, ETFE cografted with styrene and GMA, functionalized cografted film and functionalized and sulfonated ETFE-*g*-P(SSA-*co*-GMA(Tyr)) are given. After the grafting step, the combined aromatic vibration at 1600 cm^{-1} and carbonyl stretch vibration at 1720 cm^{-1} confirm the presence of both styrene and GMA in the cografted film. Additionally, the band at 910 cm^{-1} (oxirane stretch vibration) indicates the presence of intact epoxide after cografting and workup procedure. The carbonyl and oxirane bands are found in ETFE grafted with GMA only at the same wavenumers.[60] The FTIR spectrum of tyraminated film (ETFE-*g*-P(S-*co*-GMA(Tyr))) shows a new broad band at high wavenumber indicating N-H and O-H stretch vibrations from the amine and the aromatic alcohol of tyramine. Accordingly, the oxirane stretch vibration almost disappears, thus, the epoxy group is converted to amine. After sulfonation and hydrolysis of the membrane, new bands for SO_2 symmetric stretch and S-O stretch vibrations at 1010 cm^{-1} and 835 cm^{-1} appear, indicating the presence of sulfonic acid groups in the membrane.

For the baseline samples (films cografted with styrene and GMA), for which the amination of GMA was not performed, the epoxy groups of GMA disappeared after sulfonation and hydrolysis (FTIR spectra not shown here). The epoxy groups were opened to the diol, GMA(diol), which was confirmed by elemental analysis (cf. Supplementary Information). This was necessary to be able to test a chemically similar, yet non-stabilized membrane with comparable gas crossover and water uptake with respect to corresponding tyraminated membranes, GMA(Tyr). This baseline allows a more meaningful comparison

between non-stabilized and tyramine containing membranes compared to a pure styrene grafted and sulfonated membrane, ETFE-*g*-PSSA. Interestingly, the obtained IEC values of these GMA(diol) type membranes (graft levels of 35 % and 55 %) were 1.62 mmol/g and 2.09 mmol/g, corresponding to a degree of sulfonation of the styrene units of 97 % and 100 %, respectively. This confirms that the sulfonation procedure is successful for films containing GMA as linker. Additionally, it can be deduced that for VBC containing films, the VBC is sulfonated and not the tyramine, because the sulfonation procedure is the same for all films and only elemental analysis of VBC containing sulfonated films shows a sulfur content that is higher than expected.

Bulk properties of membranes

A range of fuel cell relevant *ex situ* properties of are given in Table 4: mass based swelling in water, IEC and through-plane conductivity. Water uptake is needed to provide an aqueous phase for proton conduction. The proton conductivity of membranes is strongly correlated to the water uptake of the material.[8, 49, 50] This could be an explanation for the low proton conductivity of the analyzed VBC containing membranes. The swelling of VBC containing membranes with an IEC of 1.6 mmol/g is around 20 %, whereas for GMA containing and pure styrene based membranes of similar IEC the water uptake is 35 % and 50 %, respectively. Accordingly, the proton conductivity is around 20 mS/cm for VBC containing, around 40 mS/cm for GMA containing, and 60 mS/cm for PSSA only membranes. This confirms the strong dependency of proton conductivity on water uptake of these materials. Similarly, the findings for GMA containing membranes without tyramine compared to the ones with tyramine can be explained by the lower water uptake of the latter ones. This could be a result of acid-base interactions in the tyramined membrane ($-SO_3^-\ldots H_2N^+RR'$), yet the effect is not pronounced and almost within the uncertainty of

the conductivity measurement. On the other hand, the higher polarity of diols compared to tyramine may lead to higher water uptake and proton conductivity, especially for the series at lower GL. For these films, the influence of the comonomer of styrene is more pronounced, because at higher GLs the phase separation behavior seems to be dominated by the PSSA content. In contrast, at a GL of 35 %, the influence of the hydrolyzed GMA units with diol groups, compared to the tyraminated GMA, enhances the water uptake in a more significant manner, as the concentration of PSSA in the material seems to be not yet sufficiently high to dominate the water uptake completely.

(Figure 4)

Another detrimental aspect for the durability of proton exchange membranes in fuel cells is the distribution of the sulfonic acid groups throughout the membrane material. Different swelling properties induce mechanical stress upon change of the hydration state of the polymer. Therefore, it is important to ensure a homogeneous distribution of sulfonic acid groups throughout the membrane. This was analyzed by means of SEM/EDX for the two types of linker and tyramine containing membranes. Therefore, cross-sections of these membranes were prepared as described above and the elemental distribution was visualized using energy dispersive X-ray analysis (EDX). The SEM image and the corresponding sulfur mappings confirm a homogeneous distribution of sulfur in both materials (Figure 4). Sulfur is only present in the sulfonic acid group, thus it can be concluded that the proton exchange groups are well distributed throughout both membrane materials. In case of a pronounced front mechanism, the distribution of sulfur is clearly inhomogeneous.[60] For the S-*co*-GMA(Tyr) type membrane a slight gradient can be seen. This is either an artifact (shadow effect) due to the location of the EDX detector or a true sulfur gradient resulting from the front mechanism of grafting and the short grafting

time (1 and 1.5 h for 35% and 55% graft level, respectively) Similarly, the nitrogen mappings indicate a homogeneous distribution of functionalized linkers throughout both types of membrane. This can be concluded because only the tyramine contains nitrogen. Furthermore, it can be deduced that the amine is still intact after the sulfonation and hydrolysis procedures, which are carried out after linker functionalization. These findings confirm the FTIR analysis, which is less conclusive in this context, because of superposition of important bands (N-H(σ) and O-H(σ)).

All membranes are sufficiently flexible for handling and assembling into a fuel cell. GMA containing membranes are transparent and of yellow color. This is also the case for GMA(diol) type membranes, but with almost no color. The intensity of the yellow color increases with higher content of tyramine, namely, the membranes of higher GL (55 %) are of more intense yellow color compared to the ones with a GL of 35 %.

Fuel cell tests (in situ)

The synthesized membranes were assembled in a fuel cell as described above. An accelerated chemical degradation protocol was applied to probe the chemical stability of the potentially stabilized (tyramine containing) and the non-stabilized membranes. Because of the importance of reactant crossover, which is dependant of the thickness of the material, not only PSSA type membranes but also cografted and non-functionalized membranes were tested to have a fair basis for comparison.

The polarization curves of grafted membranes containing tyramine are shown in Figure 5. For comparison, the polarization curves of ETFE-*g*-PSSA (IEC: 1.7 mmol/g) and Nafion NR212 (PFSA type membrane) are given in the same Figure. ETFE-*g*-PSSA was used as reference material for a non-crosslinked grafted membrane and NR212 as state-of-the-art benchmark.

(Figure 5)

Figure 5 shows the polarization plots of different tested membrane materials after conditioning and before the accelerated chemical degradation test. Interestingly, the membrane containing tyraminated GMA shows performance almost as good as the state-of-the-art PFSA material. Additionally, it outperforms the PSSA based membrane of similar IEC (cf. Table 4). For the VBC containing membrane (*ex situ* conductivity of 20 mS/cm) a strong drop in cell voltage with increasing current densities is observed. The HFR is considerably higher for this type of membrane (200 $m\Omega cm^2$ vs. around 65 $m\Omega cm^2$ for the other membrane materials). This confirms the findings of the *ex situ* caracterization. Additionally, the HFR increases with increasing current densities, which can be attributed to drying out of the anode side of the membrane because of poor water transport in this type of membrane (low water uptake)[74]. Another reason for the inferior performance of this membrane type may be the low mobility of the grafted chains due to π-stacking of the aromatic groups of the grafts. π -stacking of the aromatic groups occurs probably also in pure PSSA type membranes, but is partially compensated by the elevated water uptake of these materials (40-50 % vs. 20 % for VBC containing materials). An additional hint supporting this hypothesis is the lower water uptake at similar IEC for GMA(Tyr) containing membranes (GL of 35 %). They show better performance compared to PSSA only type membranes (Figure 5). The comonomer GMA contains no aromatic group, consequently the π-stacking in these materials is less pronounced and leads to higher mobility of the grafted chains containing sulfonic acid groups. This could lead to an enhanced surface transport pathway (proton transport from acid to acid, in contrast to Grotthus or vehicular transport mechanisms of protons)[75]) and, thus, to higher proton conductivity, which is confirmed by *in situ* (smaller slope of the ohmic section in the polarization curve and lower

HFR) and *ex situ* findings (higher proton conductivity at slightly lower IEC and water uptake).

It can be concluded from the polarization curves shown in Figure 5 that GMA(Tyr) and PSSA membranes show promising performance compared to commercial benchmark PFSA materials. Furthermore, HFR and cell voltage indicates better proton transport in GMA(Tyr) membranes compared to PSSA materials. VBC(Tyr) shows significantly higher HFR values, indicating poor water management properties and confirming the results of the *ex situ* charactirization.

(Table 5)

To assess the chemical stability of the various membranes, polarization curves before and after 4 h at open circuit voltage (OCV) are recorded. As mentioned above, this is an accelerated aging protocol, leading to radical attack on, and, consequently loss of the grafted chains. This lowers the proton conductivity and can be qualitatively analyzed by comparing polarization curves before and after the accelerated stress test (AST). In addition, the H_2 crossover was measured before and after the AST to assess changes in the porosity and integrity of the membrane. In Table 5, these measurements are summarized. For performance characterization, the cell voltage values were extracted from polarization curves at a current density of 1 A/cm^2. Complete polarization curves can be found in the Supplementary Information (Figures S1 and S2). In addition to membranes containing tyramine as antioxidant attached to GMA linker units (GMA(Tyr)), also membranes without tyraminated GMA were prepared, which leads to ring opening and yields a diol functional group (GMA(diol)) (cf Scheme 2). This membrane provides an adequate basis for comparison in terms of swelling behavior, thickness, proton conductivity, IEC, gas barrier properties and, in general, chemical composition of the

analyzed materials. Both GMA containing membranes (GMA(diol) and GMA(Tyr)) show slightly better initial performance compared to the PSSA only type membrane. This is another hint for increased mobility of the grafted chains, owing to the introduction of the non-aromatic comonomer GMA, as the *ex situ* characterization shows similar IEC, thickness, and / or swelling properties. The GMA based membranes (both diol and tyraminated version) with higher graft level (55 %) and increased proton conductivity show the best performance, out of the shown materials. The performance loss after the AST is most pronounced for PSSA only material. For this membrane it is not possible anymore to draw high current densities above 1.6 A/cm^2. Accordingly, the HFR is increased by a factor of 3, indicating strong membrane degradation. The GMA(diol) containing membrane of lower graft level (35 %) suffers from chemical degradation as well, to some extent. Loss of cell voltage and increase of HFR after degradation is less pronounced compared to the PSSA only type membrane. The loss of cell voltage and increase of HFR is even less pronounced for GMA(diol) type membranes of higher graft level (55 %). This could be explained with the lower gas crossover of GMA containing membranes and, by consequence, decreased degradation during OCV hold, compared to the PSSA only type membrane. The initial gas crossover of GMA containing membranes is around 20 % lower than that of the PSSA only membrane. This seems to be independent of the membrane thickness, indicating enhanced barrier properties of GMA containing membranes.

From the data shown in Table 5, it can be concluded that all tyramine-free membranes show a loss in cell voltage and a corresponding increase in HFR after the AST. It is most pronounced for PSSA only type membranes, whereas the degradation is less pronounced for both GMA(diol) containing materials. After the AST they clearly outperform the reference grafted material (PSSA only). The degradation is even less pronounced for all tyramine containing membranes. From the cell performance data in Table 5 it can be

deduced that for tyramine containing membranes the voltage loss is below 3% of the initial value, whereas the GMA(diol) membranes loose about 10 % and PSSA only type membranes more than 20 %. The HFR evolution before and after degradation is conclusive as well: for all tyramine containing membranes is remains constant, whereas it increases by 5 to 25 % for GMA(diol) and triples for PSSA only type membranes.The hydrogen crossover of a membrane usually increases during an OCV hold test, because of detachment of grafted chains and increased porosity due to dilution of the base film upon grafting. An increase in hydrogen crossover is measured for all tyramine-free membranes, whereas all chemically stabilized membranes show the opposite trend. For GMA(Tyr) the crossover after degradation is lower and VBC(Tyr) shows the same gas crossover with respect to the initially measured values. This could be a result of recombination of phenoxy radicals. For butylated phenols recombination of the phenoxy radicals is well known and proved.[32, 76]. Basically C-C, C-O and O-O coupling are possible. Which one of these reactions occurs is difficult to prove without NMR or ESR data. Nevertheless, a lower gas crossover after the chemical degradation protocol is only seen for tyramine containing membranes. Interestingly, the GMA(diol) type materials, having a chemical composition very similar to the one of GMA(Tyr), do show increased gas crossover after chemical degradation, whereas the stabilized ones have decreased crossover. Recent experiments show that a higher degree of crosslinking in a radiation grafted membrane leads to lower reaction gas crossover.[64]. The same publication shows an increase of gas crossover for crosslinked membranes after the AST.

Post-test characterization

After the test, the fuel cells were disassembled and the catalyst layer was removed from the tested membranes, as described above. This was done to determine the loss of IEC by

titration, which indicates the loss of grafted chains, as the protogenic group (-SO_3H) is attached to the grafts. The results of titration (Table 5) confirm the *in situ* results discussed in the previous sections. Almost no loss of IEC is found for GMA(Tyr) containing membranes (4 to 9%), whereas the corresponding baseline (GMA(diol)) looses about 50% of the initial IEC, indicating substantial loss of grafted chains during chemical degradation. Similarly, the VBC(Tyr) containing membranes loose 11% of the sulfonic acid groups and the most substantial loss of IEC is seen with PSSA only type membranes (66%). The results of the change in performance (*in situ*) before and after the AST and in the IEC based on the analyisis of pristine and tested membranes (*ex situ*) are summarized in Figure 6. The differences of *in situ* and *ex situ* results can be explained by already detached fragments of grafts, which are still conducting protons when present in the membranes. Before titration, these membranes are swollen in an ethanol-water mixture to facilitate the removal of the catalyst layer. During this step, probably most of detached fragments are washed out. One possibility to partially wash out fragments of grafts *in situ* is to periodically vary the current density (such as, during the recording of polarization curves) and, consequently, the electroosmotic drag. Still, the difference in subsequently recorded polarization curves is smaller compared to the change of IEC for pristine and tested membranes. This indicates that the swelling in the EtOH-water mixture is very efficient in terms of removal of detached grafted chains.

(Figure 6)

Post test FTIR analysis (cf. Supplementary Information) of the membranes confirmed the results of titration. The spectra for tyramine containing membranes are almost identical compared to the pristine membranes, whereas non-stabilized membranes showed substantial loss of graft components after AST.

Conclusion

A synthetic pathway to introduce polymer-bound antioxidants into radiation grafted fuel cell membranes is presented here. A model antioxidant, tyramine, was covalently attached to a linker monomer, which was cografted with styrene onte ETFE basefilm of 25 μm thickness. Two potential linkers, vinylbenzyl chloride (VBC) and glycidyl methacrylate (GMA) were chosen. After cografting with styrene, the linker units were functionalized with tyramine. The graft level was adjusted to achieve an ion exchange capacity (IEC) of around 1.6 mmol/g. All membranes were characterized using FTIR and SEM/EDX. Exploitable *ex situ* conductivities of 20 to 40 mS/cm were found for chemically stabilized membranes.

The radiation grafted membranes containing antioxidant functionalities were subjected to an accelerated stress test in the fuel cell to assess the effect of the attached tyramine. These chemically stabilized membranes were compared to reference grafted membranes of similar IEC and proton conductivity. All antioxidant containing membranes degraded substantially less compared to non-stabilized materials, which was shown by *in situ* (voltage loss) and *post test* analysis (IEC loss). The linker was shown to have important influence on the performance of the synthesized membranes, whereas the phenol type antioxidant was demonstrated to effectively reduce damage due to oxidative attack (loss of grafted chains). The GMA type membranes showed promising performance comparable to PFSA state-of-the-art membrane (Nafion® NR212).

Acknowlegdement

The Swiss National Science Foundation is gratefully acknowledged for financial support (project 200021_132382). The authors wish to thank L. Bonorand, Dr. G.G. Scherer and Prof. Dr. T.J. Schmidt for fruitful discussions.

References

1. M. Yoshitake and A. Watakabe, *Advances in Polymer Science*, 2008, **216**, 127-155.
2. B. Smitha, S. Sridhar and A. A. Khan, *Journal of Membrane Science*, 2005, **259**, 10-26.
3. S. Alkan-Gürsel, L. Gubler, B. Gupta and G. G. Scherer, *Advances in Polymer Science*, 2008, **215**, 157-217.
4. M. M. Nasef and O. Güven, *Progress in Polymer Science*, 2012, **37**, 1597-1656.
5. L. Wojnárovits, C. M. Földváry and E. Takács, *Radiation Physics and Chemistry*, 2010, **79**, 848-862.
6. M. M. Nasef and E.-S. A. Hegazy, *Progress in Polymer Science*, 2004, **29**, 499-561.
7. L. Gubler, *Advanced Energy Materials*, 2014, in press (DOI: 10.1002/aenm.201300827).
8. A. Chapiró, *Radiation Chemistry of Polymeric Systems*, Wiley–Interscience, New York 1962.
9. J. Dobó, A. Somogyi and T. Czvikovszky, *Journal of Polymer Science: Part C*, 1963, **4**, 1173 - 1193.
10. H. Ben youcef, L. Gubler, S. Alkan-Gürsel, D. Henkensmeier, A. Wokaun and G. G. Scherer, *Electrochemistry Communications*, 2009, **11**, 941-944.
11. R. Borup, J. Meyers, B. Pivovar, Y. S. Kim, R. Mukundan, N. Garland, D. Myers, M. Wilson, F. Garzon, D. Wood, P. Zelenay, K. More, K. Stroh, T. Zawodzinski, J. Boncella, J. E. McGrath, M. Inaba, K. Miyatake, M. Hori, K. Ota, Z. Ogumi, S. Miyata, A. Nishikata, Z. Siroma, Y. Uchimoto, K. Yasuda, K. I. Kimijima and N. Iwashita, *Chemical Reviews*, 2007, **107**, 3904-3951.
12. M. Danilczuk, A. J. Perkowski and S. Schlick, *Macromolecules*, 2009, **43**, 3352-3358.
13. P. Trogadas, J. Parrondo and V. Ramani, *Electrochemical and Solid-State Letters*, 2008, **11**, B113-B116.
14. P. Trogadas and V. Ramani, *Journal of Power Sources*, 2007, **174**, 159-163.
15. D. Zhao, B. L. Yi, H. M. Zhang, H. M. Yu, L. Wang, Y. W. Ma and D. M. Xing, *Journal of Power Sources*, 2009, **190**, 301-306.
16. L. Gubler and W. H. Koppenol, *Journal of The Electrochemical Society*, 2012, **159**, B211-B218.
17. V. O. Mittal, H. Russell Kunz and J. M. Fenton, *Electrochemical and Solid-State Letters*, 2006, **9**, A299-A302.

18. V. O. Mittal, H. R. Kunz and J. M. Fenton, *Journal of the Electrochemical Society*, 2006, **153**, A1755-A1759.

19. D. Zhao, B. L. Yi, H. M. Zhang and H. M. Yu, *Journal of Membrane Science*, 2010, **346**, 143-151.

20. V. O. Mittal, H. R. Kunz and J. M. Fenton, *Journal of the Electrochemical Society*, 2007, **154**, B652-B656.

21. J. M. Fenton, M. P. Rodgers, D. K. Slattery, X. Huang, V. O. Mittal, L. J. Bonville and H. R. Kunz, in *ECS Transactions*, 2009, pp. 233-247.

22. M. Inaba, T. Kinumoto, M. Kiriake, R. Umebayashi, A. Tasaka and Z. Ogumi, *Electrochimica Acta*, 2006, **51**, 5746-5753.

23. G. Hübner and E. Roduner, *Journal of Materials Chemistry*, 1999, **9**, 409-418.

24. S. M. Dockheer, L. Gubler and W. H. Koppenol, *Physical Chemistry Chemical Physics*, 2013, **15**, 4975-4983.

25. S. M. Dockheer, L. Gubler, A. Wokaun and W. H. Koppenol, *Physical Chemistry Chemical Physics*, 2011, **13**, 12429-12434.

26. S. M. Dockheer, L. Gubler, P. L. Bounds, A. S. Domazou, G. G. Scherer, A. Wokaun and W. H. Koppenol, *Physical Chemistry Chemical Physics*, 2010, **12**, 11609-11616.

27. L. Gubler, S. M. Dockheer and W. H. Koppenol, *Journal of the Electrochemical Society*, 2011, **158**, B755-B769.

28. M. Danilczuk, F. D. Coms and S. Schlick, *Journal of Physical Chemistry B*, 2009, **113**, 8031-8042.

29. Z. Zhang, K. Jetsrisuparb, A. Wokaun and L. Gubler, *Journal of Power Sources*, 2013, **243**, 306-316.

30. L. Gubler and L. Bonorand, *ECS Transactions*, 2013, **58**, 149-162.

31. S. Al-Malaika, in *Reactive Modifiers for Polymers*, ed. S. Al-Malaika, Chapman & Hall, London, 1997, pp. 266-302.

32. S. Steenken, in *The Chemistry of Phenols*, ed. Z. Rappoport, John Wiley & Sons Ltd., Chichester, 2003, 1107-1152.

33. T. Cohen, P. Dagard, J. Molenat, B. Brun and C. Gavach, *Journal of Electroanalytical Chemistry and Interfacial Electrochemistry*, 1986, **210**, 329-336.

34. M. N. Szentirmay and C. R. Martin, *Journal of The Electrochemical Society*, 1984, **131**, 1652-1657.

35. M. J. Sundell, K. B. Elkman, B. L. Svarfvar and J. H. Näsman, *Reactive Polymers*, 1995, **25**, 1-16.

36. A. Jyo, S. Aoki, T. Kishita, K. Yamabe, M. Tamada and T. Sugo, *Analytical Sciences/Supplements*, 2002, **17icas**, i201-i204.

37. J. R. Varcoe and R. C. T. Slade, *Electrochemistry Communications*, 2006, **8**, 839-843.

38. H. Herman, R. C. T. Slade and J. R. Varcoe, *Journal of Membrane Science*, 2003, **218**, 147-163.

39. T. N. Danks, R. C. T. Slade and J. R. Varcoe, *Journal of Materials Chemistry*, 2003, **13**, 712-721.

40. T. N. Danks, R. C. T. Slade and J. R. Varcoe, *Journal of Materials Chemistry*, 2002, **12**, 3371-3373.

41. M. Böhme, PhD Thesis, TU Clausthal, 2005.

42. G. Schmidt-Naake, M. Böhme and A. Cabrera, *Chemical Engineering & Technology*, 2005, **28**, 720-724.

43. V. Y. Kabanov, N. M. Kazimirova and V. I. Spitsyn, *Polymer Science U.S.S.R.*, 1968, **10**, 821-828.

44. K. Manaka and T. Tomioka, *Journal of Applied Polymer Science*, 1965, **9**, 3635-3648.

45. V. Y. Kabanov, N. M. Kazimirova and V. I. Spitsyn, *Polymer Science U.S.S.R.*, 1967, **9**, 1983-1990.

46. K. Saito, T. Kaga, H. Yamagishi, S. Furusaki, T. Sugo and J. Okamoto, *Journal of Membrane Science*, 1989, **43**, 131-141.

47. A. Chapiró and V. Stannett, *The International Journal of Applied Radiation and Isotopes*, 1960, **8**, 164-167.

48. A. Revillon, A. Guyot, Q. Yuan and P. da Prato, *Reactive Polymers*, 1989, **10**, 11-25.

49. A. Jyo, K. Okada, M. Tamada, T. Kurne and T. Sugo, in *Chemistry for the protection of the environment*, eds. R. Mournigham, M. R. Dudzi, J. Barich and M. A. Gonzales, Springer Science, 2005, pp. 49 - 62.

50. E. E. Abdel-Hady, M. M. El-Toony and M. O. Abdel-Hamed, *Electrochimica Acta*, 2013, **103**, 32-37.

51. X.-Z. Yuan, H. Li, S. Zhang, J. Martin and H. Wang, *Journal of Power Sources*, 2011, **196**, 9107-9116.

52. Z. Zhang, Y. Buchmüller, A. Wokaun and L. Gubler, *ECS Electrochemistry Letters*, 2013, **2**, F69-F72.

53. V. A. Sethuraman, J. W. Weidner, A. T. Haug and L. V. Protsailo, *Journal of the Electrochemical Society*, 2008, **155**, B119-B124.

54. S. Alkan-Gürsel, H. Ben youcef, A. Wokaun and G. G. Scherer, *Nuclear Instruments and Methods in Physics Research Section B: Beam Interactions with Materials and Atoms*, 2007, **265**, 198-203.

55. H.-P. Brack, H. G. Bührer, L. Bonorand and G. G. Scherer, *Journal of Materials Chemistry*, 2000, **10**, 1795-1803.

56. F. Wallasch, M. Abele, L. Gubler, A. Wokaun, K. Müller and G. G. Scherer, *Journal of Applied Polymer Science*, 2012, **125**, 3500-3508.

57. K. Jetsrisuparb, S. Balog, C. Bas, L. Perrin, A. Wokaun and L. Gubler, *European Polymer Journal*, 2014, in press (DOI: 10.1016/j.eurpolymj.2014.1001.1021.

58. Y. Buchmüller, K. Jetsrisuparb and L. Gubler, *PSI Electrochemistry - Annual Report 2011*, 2012, 13 (DOI: 10.3929/ethz-a-007047464).

59. K. Jetsrisuparb, H. Ben youcef, A. Wokaun and L. Gubler, *Journal of Membrane Science*, 2014, **450**, 28-37.

60. Y. Buchmüller, A. Wokaun and L. Gubler, *Fuel Cells*, 2013, **13**, 1177-1185.

61. Y. Buchmüller, A. Wokaun and L. Gubler, *PSI Electrochemistry - Annual Report 2012*, 2013, 11 (DOI: 10.3929/ethz-a-007047464).

62. L. Gubler, N. Prost, S. Alkan-Gürsel and G. G. Scherer, *Solid State Ionics*, 2005, **176**, 2849-2860.

63. K. Jetsrisuparb, PhD Thesis No. 21257, ETH, Zürich, 2013 (DOI: 10.3929/ethz-a-009973173).

64. L. Gubler, H. Ben youcef, S. Alkan-Gürsel, A. Wokaun and G. G. Scherer, *Journal of the Electrochemical Society*, 2008, **155**, B921-B928.

65. N. Linse, G. G. Scherer, A. Wokaun and L. Gubler, *Journal of Power Sources*, 2012, **219**, 240-248.

66. Y. Buchmüller, G. G. Scherer, A. Wokaun and L. Gubler, *PSI Electrochemistry - Annual Report 2011*, 2012, 7-8 (DOI: 10.3929/ethz-a-007047464).

67. T. Rager, *Helvetica Chimica Acta*, 2003, **86**, 1966-1981.

68. D. Stefanec and P. Krajnc, *Reactive and Functional Polymers*, 2005, **65**, 37-45.

69. E. Pretsch, P. Bühlmann, C. Affolter and M. Badertscher, *Spektroskopische Daten zur Strukturaufklärung organischer Verbindungen*, Springer-Verlag, Berlin Heidelberg New York, 2001.

70. Y. Buchmüller, A. Wokaun and L. Gubler, in *IRaP 2012, Book of abstracts*, Crakow, Poland, 2012.

71. M. M. Nasef, H. Saidi and K. Z. M. Dahlan, *Journal of Membrane Science*, 2009, **339**, 115-119.

72. L. Gubler, M. Slaski, F. Wallasch, A. Wokaun and G. G. Scherer, *Journal of Membrane Science*, 2009, **339**, 68-77.

73. M. M. Nasef, N. A. Zubir, A. F. Ismail, M. Khayet, K. Z. M. Dahlan, H. Saidi, R. Rohani, T. I. S. Ngah and N. A. Sulaiman, *Journal of Membrane Science*, 2006, **268**, 96-108.

74. F. N. Büchi and G. G. Scherer, *Journal of the Electrochemical Society*, 2001, **148**, A183-A188.

75. T. J. Peckham and S. Holdcroft, *Advanced Materials*, 2010, **22**, 4667-4690.

76. K. Omura, *Tetrahedron*, 1995, **51**, 6901-6910.

Tables

Table 1. Synthetic parameters for (co)grafting of different (co)monomers into ETFE.

Monomer(s)	Dose / kGy	Temperature /°C	Time / h	Monomer(s) conc in solvent (v/v)	Monomers ratio (v/v)	Solvent(s)	Solvents ratio (v/v)
S	1.5	60	1	1 / 4	-	^{i}PrOH / water	7 / 1
VBC	30	60	varying	1 / 1	-	DMF	-
GMA	15	60	varying	1 / 9	-	MeOH	-
S / VBC	30	60	20	1 / 1	1 / 1	DMF	-
S / GMA	15	60	varying	1 / 4	1 / 1	^{i}PrOH	-
S / GMA	15	60	1 and 1.5	1 / 4	7 / 3	^{i}PrOH	-

Table 2. Compositional analysis of ETFE cografted with S and GMA. X_S is the molar fraction of styrene in the grafts (thus, 1-X_S is the molar fraction of GMA).

ETFE-*g*-	X_S (mol%) in solution	X_S (mol%) in grafts	GL_S (FTIR)	GL_{GMA} (FTIR)	GL_{tot} (FTIR)	GL (m%)
S-*co*-GMA(Tyr)	54	60 ± 3	18	16	34	33
S-*co*-GMA(Tyr)	54	60 ± 3	19	17	37	34
S-*co*-GMA(Tyr)	54	60 ± 3	26	25	51	47
S-*co*-GMA(Tyr)	54	60 ± 3	24	26	50	49
S-*co*-GMA(Tyr)	73	73 ± 2	21	10	31	31
S-*co*-GMA(Tyr)	73	73 ± 2	26	13	39	37
S-*co*-GMA(Tyr)	73	73 ± 2	36	19	55	54
S-*co*-GMA(Tyr)	73	73 ± 2	34	20	54	54

Table 3. Conversion of amination reaction for different films containing linkers.

ETFE-*g*-P()	Graft level (m%)	X_S (mol%) in grafts	X_{linker} (mol%) in grafts	GL_S (FTIR)	GL_{linker} (FTIR)	Conversion amination reaction (%)
VBC	44.5	0	1	0	44.5	50 ± 5
GMA	37.9	0	1	0	37.9	57.2 / 57.2
S-*co*-VBC	67.0 ± 0.8	61 ± 3	39 ± 3	31	36	25 ± 1
S-*co*-GMA	37 / 55	73 ± 2	27 ± 2	26 / 34	13 / 20	58.8 ± 0.6

Table 4. *Ex situ* properties for the different radiation grafted, post-functionalized and sulfonated membranes. Water uptake and conductivity values measured in water swollen state at room temperature.

ETFE-*g*-P()	Graft level	X_S (mol%)	IEC (mmol/g)	Water uptake (m%)	Hydration (H_2O / SO_3H)	Thickness (wet) (μm)	Conductivity (mS/cm)
S	25	100	1.73 ± 0.13	50 ± 4	15.9 ± 0.6	38.2 ± 1.1	58 ± 4
S / VBC(Tyr)	66	62 ± 2	1.63 ± 0.06	20 ± 6	7.2 ± 2.3	42.9 ± 1.2	21 ± 2
S / GMA(Tyr)	35	60 ± 3	1.62 ± 0.05	35 ± 3	12.0 ± 0.9	39.1 ± 1.1	41 ± 10
S / GMA(Tyr)	55	68 ± 3	1.99 ± 0.01	52 ± 3	14.6 ± 0.9	48.1 ± 0.8	100 ± 10
S / GMA(diol)	35	60 ± 3	1.62 ± 0.02	43 ± 2	14.8 ± 0.6	41.1 ± 1.2	66 ± 7
S / GMA(diol)	55	68 ± 3	2.09 ± 0.07	64 ± 11	16.9 ± 2.6	44.2 ± 1.3	91 ± 11
Nafion NR212	-	-	1.08 ± 0.01	42 ± 1	21.6 ± 0.8	64.0 ± 1.2	97 ± 15

Table 5. *Cell voltage and high frequency resistance (HFR) at 1 kHz measured at a current density of 1 A/cm^2, H_2 crossover and IEC values of different tested membranes before and after* in situ *chemical degradation (AST = accelerated stress test). The* post-test *IEC values for the repeat expeiments are given.*

ETFE-*g*-P()	Graft level	IEC (mmol/g)	Cell voltage		HFR		H_2 crossover		IEC	
			before AST (mV)	after AST (mV)	before AST (mΩcm^2)	after AST (mΩcm^2)	before AST (ml/min)	after AST (ml/min)	after AST (mmol/g)	loss (%)
SSA	25	1.73 ± 0.13	693	526	62	186	0.19 ± 0.02	0.24 ± 0.03	0.58 ± 0.04	66 ± 2
SSA-*co*-VBC(Tyr)	67.0	1.63 ± 0.06	557	540	246	247	0.07 ± 0.01	0.07 ± 0.01	1.45 ± 0.12 / 1.45 ± 0.06	11 / 11
SSA-*co*-GMA(Tyr)	34.6	1.62 ± 0.05	724	713	68	68	0.15 ± 0.01	0.13 ± 0.01	1.53 ± 0.06 / 1.47 ± 0.06	6 / 9
SSA-*co*-GMA(Tyr)	56.8	2.06 ± 0.05	714	717	62	62	0.12 ± 0.01	0.10 ± 0.00	1.97 ± 0.05 / 1.98 ± 0.04	4 / 4
SSA-*co*-GMA(diol)	32.2	1.45 ± 0.02	712	658	74	96	0.15 ± 0.00	0.19 ± 0.00	0.71 ± 0.08 / 0.87 ± 0.11	51 / 46
SSA-*co*-GMA(diol)	56.3	2.09 ± 0.07	711	668	55	58	0.16 ± 0.00	0.23 ± 0.01	0.92 ± 0.03 / 0.91 ± 0.07	56 / 56

Schemes and Figures

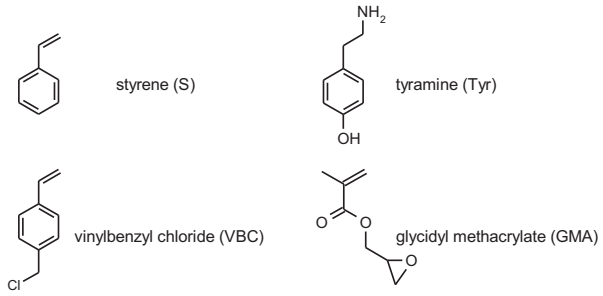

Scheme 1. *Grafting monomers and radical scavenger (antioxidant) used in this study.*

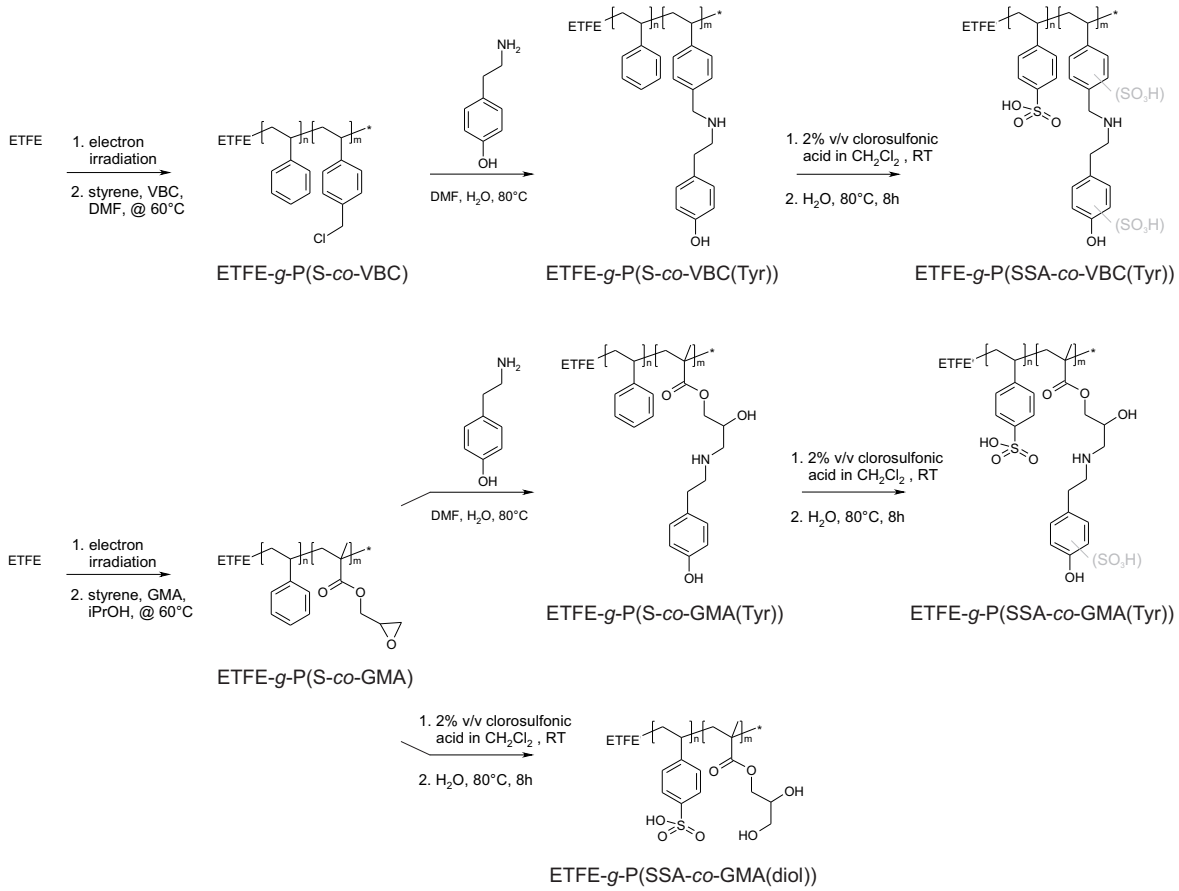

Scheme 2. *Reaction schemes for synthesizing radiation grafted membranes for fuel cells with antioxidant functionality provided by tyramine, based on vinylbenzene chloride (VBC) and glycidyl methacrylate (GMA) as linker, respectively. Potential sulfonation of the aromatic ring of VBC and tyramine is indicated in gray. For comparison reasons, the styrene / GMA cografted membrane is also sulfonated directly without prior tyramination, yielding the diol compound.*

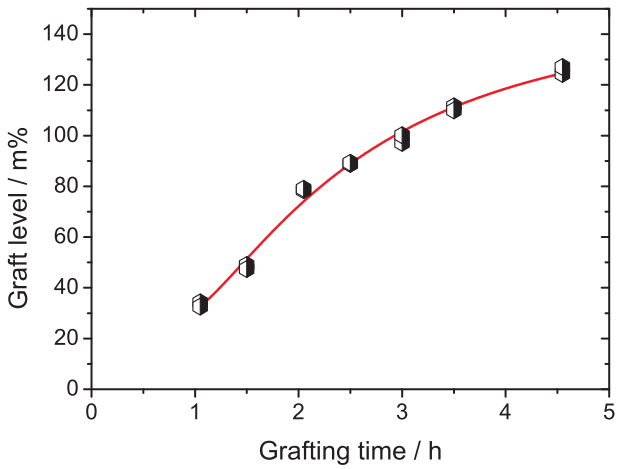

Figure 1. *Reaction kinetics for cografting of styrene and GMA (1 / 1)(v / v) into ETFE.*

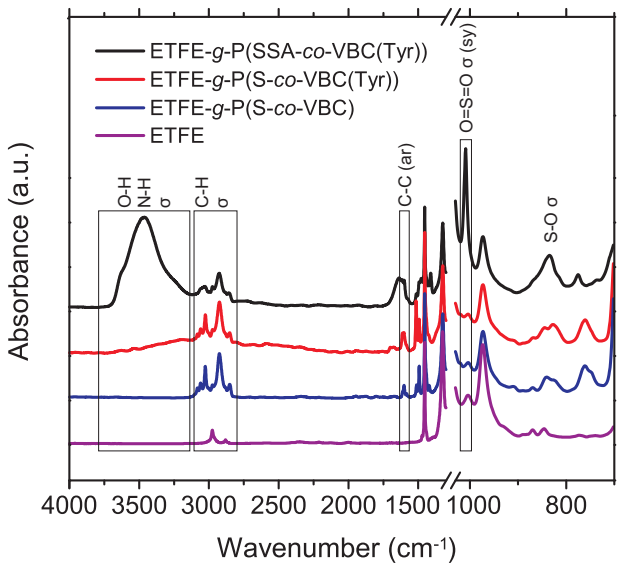

Figure 2. *FTIR spectra of pristine ETFE, ETFE cografted with styrene and VBC (1/1)(v/v), functionalized cografted film (ETFE-*g*-P(S-*co*-VBC(Tyr))) and VBC(Tyr) type membrane after sulfonation (ETFE-*g*-P(SSA-co-VBC(Tyr)).*

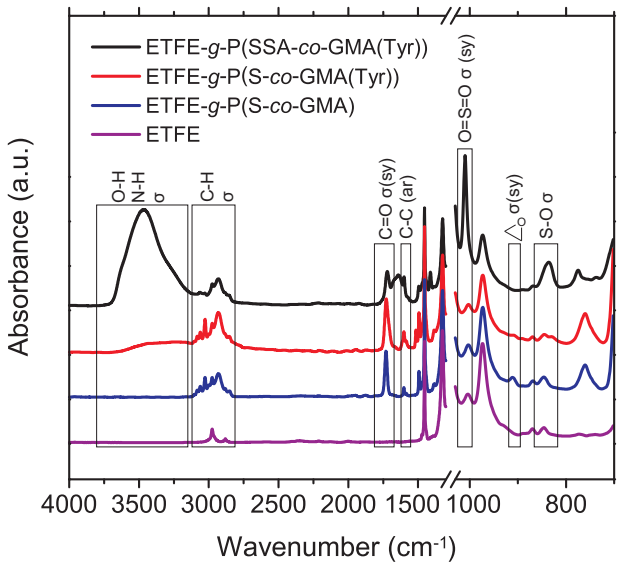

Figure 3. *FTIR spectra of pristine ETFE, ETFE cografted with styrene and GMA (7/3)(v/v), functionalized cografted film (ETFE-*g*-P(S-co*GMA(Tyr))) *and GMA(Tyr) type membrane after sulfonation (ETFE-*g*-P(SSA-co-GMA(Tyr))).*

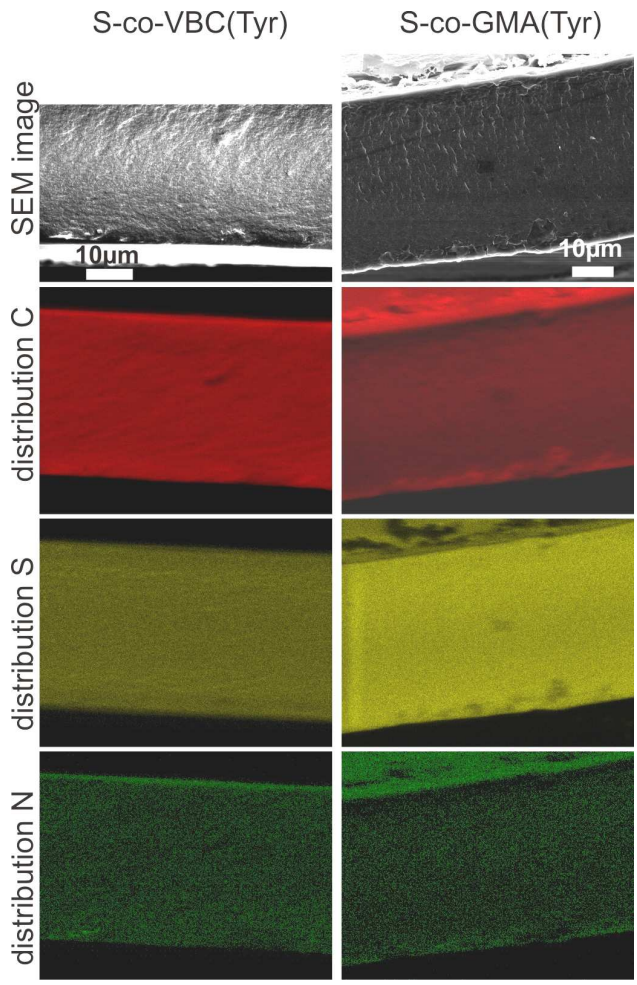

Figure 4. *Distribution of C, S and N in functionalized and sulfonated membranes (containing linked antioxidants). Sulfur indicates the distribution of sulfonic acid groups and nitrogen indicates the distribution of attached antioxidant (tyramine) throughout the membrane.*

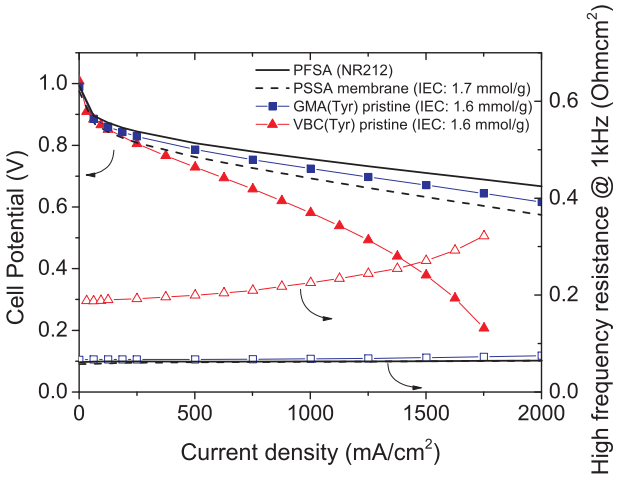

Figure 5. *Initial polarization curves of different radiation grafted membranes containing antioxidants compared to reference grafted membane (PSSA) and to state of the art PFSA membrane. All grafted membranes have similar IEC values to be comparable.*

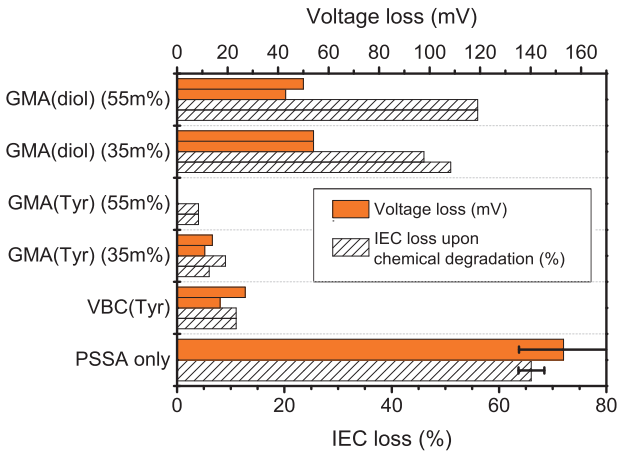

Figure 6. *Loss of IEC (*ex situ*) and loss of cell voltage at 1 A/cm^2 (*in situ*) after the accelerated degradation test (80°C, 4 h at OCV, 600 ml/min of H_2 and O_2 at 100 % r.h., 2.5 bar$_a$ gas pressure) of chemically stabilized (tyramine containing) and reference grafted membrane materials (five PSSA only type membranes were tested and analyzed). No* in situ *voltage loss was observed for GMA(Tyr) of a graft level of 55%.*